The nanotube oscillator parameters presented above are representative of all of our measured devices. Using these parameters, we can calculate the force sensitivity of the device at room temperature. The smallest detected motion of the nanotube was at a resonant driving voltage of $\delta V_g \approx 1$ mV in the bandwidth of 10 Hz. The sensitivity was limited by the Johnson–Nyquist electronic noise from the nanotube. Using equations (1) and (3) above, this corresponds to a motion of ~0.5 nm on resonance and a force sensitivity of $\sim 1\,\mathrm{fN\,Hz^{-1/2}}$. This is within a factor of ten of the highest force sensitivities measured at room temperature[24].

The ultimate limit on force sensitivity is set by the thermal vibrations of the nanotube. The corresponding force sensitivity is $\delta F_{\min} = \sqrt{\frac{4k_B kT}{\omega_0 Q}} = 20\,\mathrm{aN\,Hz^{-1/2}}$ for typical parameters. The observed sensitivity is 50 times lower than this limit. This is probably due to the relatively low values of transconductance for the measured nanotubes at room temperature. At low temperatures (~1 K), the sensitivity should increase by orders of magnitude owing to the high transconductance associated with Coulomb oscillations[19]. Even without increasing Q, force sensitivities below 5 aN should theoretically be attainable at low temperatures. This is comparable to the highest sensitivities measured[25–28]. The combination of high sensitivity, tunability, and high-frequency operation make nanotube oscillators promising for a variety of scientific and technological applications. □

Received 29 April; accepted 29 July 2004; doi:10.1038/nature02905.

1. Sidles, J. A. *et al.* Magnetic-resonance force microscopy. *Rev. Mod. Phys.* **67,** 249–265 (1995).
2. Roukes, M. Plenty of room indeed. *Sci. Am.* **285,** 48–57 (2001).
3. Nguyen, C. T. C. Frequency-selective MEMS for miniaturized low-power communication devices. *IEEE Trans. Microwave Theory Tech.* **47,** 1486–1503 (1999).
4. Nguyen, C. T. C., Wong, A.-C. & Hao, D. *Solid-State Circuits Conf. 78–79, 1999* (Digest of Technical Papers, ISSCC, IEEE International, San Francisco, California, 1999).
5. Cho, A. Physics—Researchers race to put the quantum into mechanics. *Science* **299,** 36–37 (2003).
6. LaHaye, M. D., Buu, O., Camarota, B. & Schwab, K. C. Approaching the quantum limit of a nanomechanical resonator. *Science* **304,** 74–77 (2004).
7. Dresselhaus, M. S., Dresselhaus, G. & Avouris, P. *Carbon Nanotubes* (Springer, Berlin, 2001).
8. Poncharal, P., Wang, Z. L., Ugarte, D. & de Heer, W. A. Electrostatic deflections and electromechanical resonances of carbon nanotubes. *Science* **283,** 1513–1516 (1999).
9. Gao, R. P. *et al.* Nanomechanics of individual carbon nanotubes from pyrolytically grown arrays. *Phys. Rev. Lett.* **85,** 622–625 (2000).
10. Reulet, B. *et al.* Acoustoelectric effects in carbon nanotubes. *Phys. Rev. Lett.* **85,** 2829–2832 (2000).
11. Purcell, S. T., Vincent, P., Journet, C. & Binh, V. T. Tuning of nanotube mechanical resonances by electric field pulling. *Phys. Rev. Lett.* **89,** 276103 (2002).
12. Babic, B., Furer, J., Sahoo, S., Farhangfar, S. & Schonenberger, C. Intrinsic thermal vibrations of suspended doubly clamped single-wall carbon nanotubes. *Nano Lett.* **3,** 1577–1580 (2003).
13. Minot, E. D. *et al.* Tuning carbon nanotube band gaps with strain. *Phys. Rev. Lett.* **90,** 156401 (2003).
14. Kong, J., Soh, H. T., Cassell, A. M., Quate, C. F. & Dai, H. J. Synthesis of individual single-walled carbon nanotubes on patterned silicon wafers. *Nature* **395,** 878–881 (1998).
15. Hertel, T., Walkup, R. E. & Avouris, P. Deformation of carbon nanotubes by surface van der Waals forces. *Phys. Rev. B* **58,** 13870–13873 (1998).
16. Tans, S. J., Verschueren, A. R. M. & Dekker, C. Room-temperature transistor based on a single carbon nanotube. *Nature* **393,** 49–52 (1998).
17. Zhou, C. W., Kong, J. & Dai, H. J. Intrinsic electrical properties of individual single-walled carbon nanotubes with small band gaps. *Phys. Rev. Lett.* **84,** 5604–5607 (2000).
18. Minot, E. D., Yaish, Y., Sazonova, V. & McEuen, P. L. Determination of electron orbital magnetic moments in carbon nanotubes. *Nature* **428,** 536–539 (2004).
19. Knobel, R. G. & Cleland, A. N. Nanometre-scale displacement sensing using a single electron transistor. *Nature* **424,** 291–293 (2003).
20. Brenner, D. W. Empirical potential for hydrocarbons for use in simulating the chemical vapor-deposition of diamond films. *Phys. Rev. B* **42,** 9458–9471 (1990).
21. Sapmaz, S., Blanter, Y. M., Gurevich, L. & van der Zant, H. S. J. Carbon nanotubes as nanoelectromechanical systems. *Phys. Rev. B* **67,** 235414 (2003).
22. Yurke, B., Greywall, D. S., Pargellis, A. N. & Busch, P. A. Theory of amplifier-noise evasion in an oscillator employing a nonlinear resonator. *Phys. Rev. A.* **51,** 4211–4229 (1995).
23. Bhiladvala, R. B. & Wang, Z. J. Effect of fluids on the Q-factors and resonance frequency of oscillating beams. *Phys. Rev. E* **69,** 036307 (2004).
24. Jenkins, N. E. *et al.* Batch fabrication and characterization of ultrasensitive cantilevers with submicron magnetic tips. *J. Vac. Sci. Technol. B* **22,** 909–915 (2004).
25. Stowe, T. D. *et al.* Attonewton force detection using ultrathin silicon cantilevers. *Appl. Phys. Lett.* **71,** 288–290 (1997).
26. Mohanty, P., Harrington, D. A. & Roukes, M. L. Measurement of small forces in micron-sized resonators. *Physica B* **284,** 2143–2144 (2000).
27. Stipe, B. C., Mamin, H. J., Stowe, T. D., Kenny, T. W. & Rugar, D. Magnetic dissipation and fluctuations in individual nanomagnets measured by ultrasensitive cantilever magnetometry. *Phys. Rev. Lett.* **86,** 2874–2877 (2001).
28. Mamin, H. J. & Rugar, D. Sub-attonewton force detection at millikelvin temperatures. *Appl. Phys. Lett.* **79,** 3358–3360 (2001).

Acknowledgements We thank E. Minot for discussions. This work was supported by the NSF through the Cornell Center for Materials Research and the NIRT program, and by the MARCO Focused Research Center on Materials, Structures, and Devices. Sample fabrication was performed at the Cornell Nano-Scale Science and Technology Facility (a member of the National Nanofabrication Infrastructure Network), funded by the NSF.

Competing interests statement The authors declare that they have no competing financial interests.

Correspondence and requests for materials should be addressed to P.L.M. (mceuen@ccmr.cornell.edu).

Supramolecular self-assembled molecules as organic directing agent for synthesis of zeolites

Avelino Corma[1], Fernando Rey[1], Jordi Rius[2], Maria J. Sabater[1] & Susana Valencia[1]

[1]*Instituto de Tecnología Química, UPV-CSIC, Universidad Politécnica de Valencia, Avda de los Naranjos s/n, 46022 Valencia, Spain*
[2]*Institut de Ciència de Materials de Barcelona (CSIC), Campus de la UAB, 08193 Bellaterra, Catalunya, Spain*

Solid materials with uniform micropores, such as zeolites, can act as selective catalysts and adsorbents for molecular mixtures by separating those molecules small enough to enter their pores while leaving the larger molecules behind[1,2]. Zeolite A is a microporous material with a high void volume. Despite its widespread industrial use in, for example, molecular separations and in detergency[3,4], its capability as a petroleum-refining material is limited owing to its poor acid-catalytic activity and hydrothermal stability, and its low hydrophobicity. These characteristics are ultimately a consequence of the low framework Si/Al ratio (normally around one) and the resulting high cationic fraction within the pores and cavities[1,2]. Researchers have modified the properties of type-A zeolites by increasing the Si/Al compositions up to a ratio of three[5–9]. Here we describe the synthesis of zeolite A structures exhibiting high Si/Al ratios up to infinity (pure silica). We synthesize these materials, named ITQ-29, using a supramolecular organic structure-directing agent obtained by the self-assembly, through π–π type interactions, of two identical organic cationic moieties. The highly hydrophobic pure-silica zeolite A can be used for hydrocarbon separations that avoid oligomerization reactions, whereas materials with high Si/Al ratios give excellent shape-selective cracking additives for increasing propylene yield in fluid catalytic cracking operations. We have also extended the use of our supramolecular structure-directing agents to the synthesis of a range of other zeolites.

Zeolite A has an 'LTA' structure[10], which can be envisaged as a three-dimensional network of spherical ~1.14 nm cavities (α-cages), interconnected by six small windows that are limited by eight-membered ring (8MR) pores with a diameter of 0.41 nm (see Fig. 1). This structure can also be described in terms of sodalite cages (β-cages), which are connected through the square faces with each other, forming double four-ring units (D4R). Typically, it is synthesized in the sodium form with framework Si/Al ratios of about one, the composition of the unit cell being: $[Na_{12}Al_{12}Si_{12}O_{48}]\cdot(H_2O)_{27}$. The adsorption capacity of this zeolite can be increased by replacing the sodium with calcium cations in a post-synthesis exchange. The calcium form of zeolite A (CaA) already shows good adsorption selectivity that allows the normal

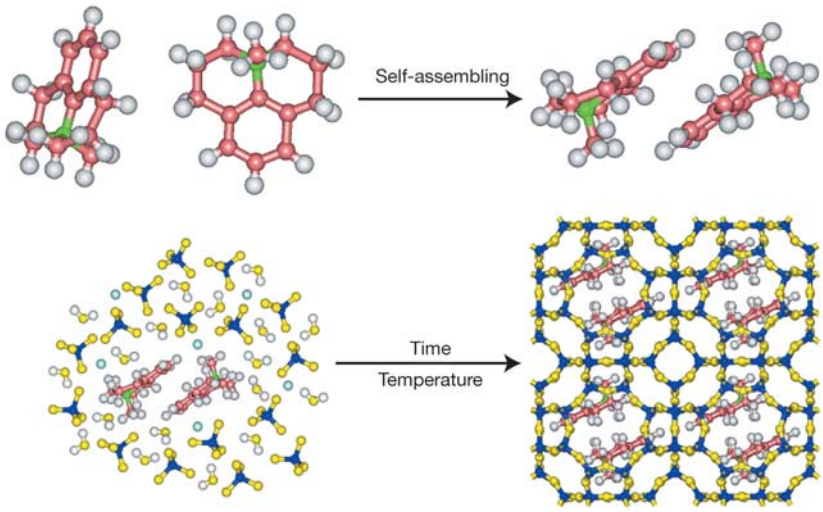

Figure 1 Formation of the LTA structure from the supramolecular self-assembling of the OSDA molecules. See Supplementary Data. Atoms are colour-coded as follows: dark blue, silicon; light blue, fluorine; yellow, oxygen; red, carbon; green: nitrogen; grey, hydrogen.

short-chain alkanes to be separated from the branched ones, because the size of the 8MR windows gives access to the cavities. However, because of the polarity of CaA, this zeolite cannot be used for olefin/paraffin separations, which require a pure-silica A zeolite. Furthermore, CaA has a limited hydrothermal and acid stability that would be much improved if this zeolite could be prepared with high Si/Al ratios.

It should be possible to extend the adsorption sieving effect of zeolite A to shape selective catalysis if we could introduce acid sites into the structure. Unfortunately, a material with an Si/Al ratio of ~1 is not stable enough to support acidity.

It is not surprising that many researchers, especially those from industry, have attempted to synthesize materials having an LTA structure with higher Si/Al ratios. A partial success was achieved by researchers from Union Carbide and Mobil[5–8], who obtained zeolites with LTA structure and an Si/Al ratio up to about three by using tetramethylammonium cations (TMA^+), together with sodium ions. They realized that by filling the void volume of the zeolite with large TMA^+ cations, a limitation on the number of tetrahedral aluminium ions in the lattice should occur. Interestingly, the sodium form of those samples, despite its still low Si/Al ratio, showed improved adsorption properties. Furthermore, zeolite A with an Si/Al ratio of three already presented some possibilities for the selective hydrogenation of olefins and hydrocracking of alkanes[9], but its stability and high Al content was still not sufficient to allow some selective adsorptions and many potential catalytic applications.

To increase further the framework Si/Al ratio, it would be necessary to find bulky organic structure-directing agents (OSDA) that can fit within the zeolite cavity. A successful OSDA should have only a weak tendency to form complexes with the solvent[11,12]. Moreover, it should fit the inner surface of the cage of the LTA structure with as many van der Waals contacts as possible, but with the least deformation. Finally, the OSDA has to maintain adequate hydrophobicity. It is more difficult to achieve all these requirements simultaneously when a large organic structure-directing agent has to be prepared that will fit within an already pre-selected cavity shape. In the case of zeolite A, finding an adequate OSDA was made more difficult by the fact that the spherical shape of the cavity is delimited by small 8MR pores, and the requirement of a relatively rigid organic molecule would involve clathrasils as competing phases. Furthermore, if the hydrophobicity is inadequate and the organic–inorganic interactions are not optimal, then the structure-directing effects of the organic will not be determinant, and amorphous material could be the competing phase.

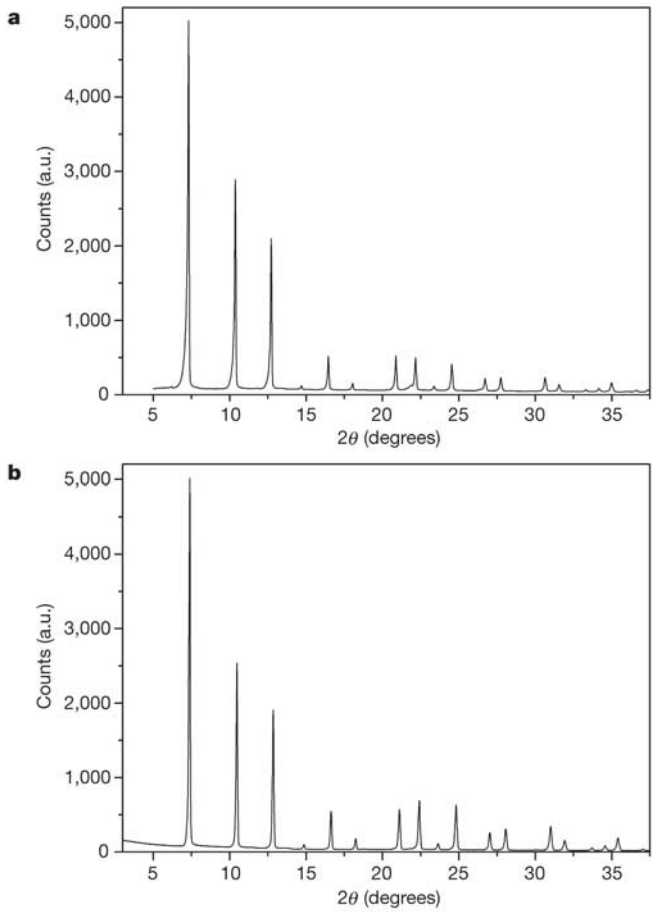

Figure 2 X-ray diffraction patterns of calcined ITQ-29 materials. **a**, Ge-contaning zeolite (Si/Ge = 2). **b**, Pure-silica zeolite.

To overcome the above limitations we used the following strategy. From our previous work[13–16], we learned that Ge, as well as F^-, can direct the synthesis towards the formation of D4R-containing structures. In fact, ITQ-21, with its six 12MR circular windows,

Table 1 **Adsorption properties of ITQ-29 compared with other zeolites**

Sample	Propane ($mg\,g^{-1}$) 298 K	313 K	333 K	Propene ($mg\,g^{-1}$) 298 K	313 K	323 K	333 K	Butane ($mg\,g^{-1}$) 353 K	Butene ($mg\,g^{-1}$) 353 K	Hexane ($mg\,g^{-1}$) 353 K	1-Hexene ($mg\,g^{-1}$) 333 K	3-Methylpentene ($mg\,g^{-1}$) 298 K	H_2O ($mg\,g^{-1}$) 298 K	Ar ($cm^3\,g^{-1}$) 87 K
ITQ-29	95	88	75	105	92	88	83	86	105	88	154	1	10	0.24
Ca-A	–	132 (ref. 23; 323 K)	–	–	–	142 (ref. 23)	–	87 (ref. 1; 348 K)	–	122 (ref. 1; 323 K)	–	–	260	0.22
ITQ-3	–	–	30 (ref. 21; 353 K)	–	61	–	53	–	–	–	–	–	–	0.23
ITQ-12	17 (ref. 22; 303 K)	–	–	55 (ref. 22; 303 K)	–	–	–	–	–	–	–	–	–	0.13

Temperatures at which the measurement was made are shown in parentheses.

Table 2 **Catalytic properties of ITQ-29 compared with other zeolites**

Catalyst	T(IV)/Al	Crystal size (μm)	Cracking kinetic constant ($10^{-2}\,s^{-1}$) 1-hexene	4-methyl-1-pentene	Methanol to olefins Conversion (%)	Ethylene/propylene
ITQ-29	20	0.6	13.0	5.4	42.1	1.0
ZSM-5	40	0.5	21.4	15.1	–	–
ITQ-3	30	0.5 × 1.5	1.8	1.8	40.4	0.5
ITQ-12	180		0.4	0.4	0	–

T(IV)/Al, ratio of tetrahedral atom to Al in catalyst.

resembles zeolite A except that the cages of ITQ-21 are not sodalite cages. Thus, at least initially, we decided to introduce Ge into the gel and to work in F^- media. This should help to link the sodalite cages, forming the corresponding D4R units that will direct the synthesis towards the LTA structure instead of the sodalite (see Fig. 1).

For the OSDA, we wanted to maximize the size to charge ratio of the organic ammonium cation, trying to reach the limit for a pure T(IV) LTA, where T(IV) indicates the element in the tetrahedral lattice with oxidation number 4. We were not able to envisage a bulky molecule that would adapt to the cavity while fulfilling the requirements for a successful template described above. We therefore started with the concept that a very large OSDA can be obtained by supramolecular self-assembling of two moieties, each with the proper rigidity and polarity properties. Of course, we could not make use of hydrogen-bonding interactions to achieve the supramolecular self-assembling because the synthesis is carried out in aqueous media. However, perhaps π–π-type interactions could be used to assemble the two starting organic molecules. If so, such an assembly method may have another benefit: by disassembling the two molecules when the synthesis is finished, the OSDA could be recovered, if the pore dimensions allow them to diffuse out[17]. Recovery, however, will not be possible in the case of the LTA structure having the large cavity connected by small pores.

Among different organic molecules considered, one of them, the 4-methyl-2,3,6,7-tetrahydro-1H,5H-pyrido [3.2.1-ij] quinolinium iodide (Fig. 1) was able to self-assemble, forming dimers—as deduced from its structural elucidation using single crystal X-ray diffraction (see Supplementary Information part 1). The ability of this OSDA to self-assemble was further studied with photoluminescence spectroscopy. We found that the main emission band in the spectrum of the aqueous solution of the OSDA in the hydroxide form used for the synthesis of ITQ-29 zeolites appears at ~450 nm (its spectrum is nearly identical to that of the solid iodide salt). The presence of this band has been observed previously when π stacking of aromatic rings in polymers occurs[18]. These results clearly indicate that the OSDA is forming self-assembled dimers in aqueous solution. Also, the same emission band was detected in the synthesized ITQ-29 zeolite (see Supplementary Information part 2). With this OSDA, Al-free ITQ-29 was synthesized (yield > 90%) with a Si/Ge = 2 (synthesis details are given in Supplementary Information part 3), and the powder X-ray diffraction (XRD) pattern of the calcined sample is given in Fig. 2a. From this, the LTA crystalline structure of ITQ-29 was confirmed. The XRD pattern was indexed according to a cubic unit cell with refined cell parameter equal to 1.20157(4) nm, where parentheses indicate uncertainty in the last digit. For the Rietveld refinement, the LTA zeolite structure type with *Pm3m* space group symmetry was employed. According to the refined scattering powder at the T site and assuming that it is filled, the unit-cell composition of the calcined sample is $Si_{16.6}Ge_{7.4}O_{48}$; that is, the refined Si/Ge ratio is 2.2 (Rietveld refinement details are given in Supplementary Information part 4).

The chemical analysis, ^{13}C–cross polarization-magic angle spinning–nuclear magnetic resonance (^{13}C–CP–MAS–NMR) and photoluminescence spectroscopies of the sample confirm that there are two intact molecules of OSDA, which are forming self-assembled dimers, within the α-cage. The charges associated with the two molecules are neutralized by two F^- ions, which are located in the D4R—as evidenced by ^{19}F MAS–NMR spectroscopy (resonances at −8 and −20 p.p.m.)[19,20].

With the synthesis procedure described above, it was possible to introduce Al (T(IV)/T(III) = 80), and ^{27}Al MAS–NMR shows that it is tetrahedrally coordinated (signal at 52 p.p.m.), suggesting that it has been incorporated in framework positions. To further decrease the framework Si/Al ratio, TMA^+ were also incorporated in the synthesis gel to compensate the framework charges generated by the introduction of Al. In this way, ITQ-29 with a T(IV)/T(III) ratio of 13 and a Si/Ge ratio of two has been synthesized, in which the Al is tetrahedrally coordinated (details are given in Supplementary Information part 3).

We emphasize that by using both TMA^+ and the quinolinium derivative OSDA it is also possible to synthesize pure-silica ITQ-29 (see Supplementary Information part 3 for detailed conditions). The powder-XRD pattern of the calcined sample is given in Fig. 2b, and from this the cubic LTA structure was confirmed, with a parameter of 1.18671(4) nm (for Rietveld refinement, see Supplementary Information part 4).

The pure-silica ITQ-29 sample is very stable and the structure is maintained after calcination at 900 °C in the presence of atmospheric moisture. The sample is also stable when treated in an aqueous solution of HCl at pH = 1. By following this approach, ITQ-29 can also be synthesized as aluminosilicate (details are given in Supplementary Information part 3).

We have measured the adsorption capacity of the pure-silica ITQ-

29 described here, the results are given in Table 1 and compared with those reported for ITQ-3 and ITQ-12 and CaA zeolites[1,21–23]. The water adsorption isotherms on CaA and pure-silica ITQ-29 at 20 mbar give 26 wt% and 1 wt% H_2O adsorption capacity, respectively, indicating the hydrophobic character of this pure-silica material. As we expected, this zeolite allows us to separate normal from branched paraffins, as can be seen in Table 1. The adsorption capacities are CaA > ITQ-29 > ITQ-3 ≫ ITQ-12. For olefin adsorption, it should be taken into account that olefin oligomerization occurs on CaA sample at the adsorption temperature[24], making this zeolite unsuitable for adsorbing olefins. In contrast, no oligomerization was detected on ITQ-29 and the adsorption capacity remains constant after 20 adsorption–desorption cycles.

Al-containing ITQ-29 zeolites show acid hydroxyl groups at 3,620 and 3,550 cm^{-1} in the infrared spectra. They are catalytically active and the results (Table 2) show a larger diffusion shape selectivity for cracking of 1-hexene and 4-methyl-1-pentene than ZSM-5, which is the commercial catalyst used for the selective cracking of lineal olefins in FCC, and for hydrocracking (dewaxing) of alkanes. Also, the cracking activity of the Al-containing ITQ-29 sample was much higher than that of other small-pore zeolites such as ITQ-3 and ITQ-12. For conversion of methanol to olefins, both ITQ-29 and ITQ-3 are active and selective catalysts, but the second zeolite shows a deactivation rate twice that of ITQ-29. In contrast, ITQ-12 presents a negligible activity owing to the impossibility of preparing this zeolite with a T(IV)/Al ratio lower than 180.

Thus we have shown that by using OSDA in a new way that involves the supramolecular self-assembling of two organic moieties, it has been possible to synthesize the Al-free as well as the pure-silica zeolites with the LTA structure. The latter is a very stable and hydrophobic material and could be used for gas separation in the presence of H_2O or other polar molecules. By introducing Al in framework positions we have been able to produce acid catalysts that give excellent shape selectivity for cracking (preferably lineal rather than branched) olefins. Such catalysts may be useful as an additive for increasing propylene yield in fluid catalytic cracking operations. Moreover, ITQ-29 may be an interesting catalyst for converting methanol into olefins. □

Methods

Synthesis of ITQ-29 zeolites

ITQ-29 zeolites were synthesized in fluoride media from gels of the following general molar compositions: $(1-x)SiO_2$: $xGeO_2$:yAl_2O_3: 0.5ROH:0.5HF: zH_2O $(1-x)SiO_2$:$xGeO_2$:yAl_2O_3:0.25ROH:0.25TMAOH:0.5HF:$zH_2O$where x was varied from 0 to 0.33, y from 0 to 0.07 and z from 2 to 7.

The gels were prepared by hydrolysing tetraethylorthosilicate (TEOS) and aluminium isopropoxide in an aqueous solution of 4-methyl-2,3,6,7-tetrahydro-1H,5H-pyrido[3.2.1-ij] quinolinium hydroxide (ROH) and tetramethylammonium hydroxide (TMAOH), then the appropriate amount of GeO_2 was added and the mixture was stirred until the ethanol formed upon hydrolysis of TEOS and the appropriate excess of water were evaporated to reach the gel composition given above. Finally, an aqueous solution of HF (50%) was added and the mixture was introduced in a Teflon-lined stainless autoclave and heated at 408 or 423 K for times of between 2 and 7 days. Then, the autoclave was cooled down, and the mixture was filtered, washed with distilled water and dried at 100 °C. The preparation of the of 4-methyl-2,3,6,7-tetrahydro-1H,5H-pyrido[3.2.1-ij] quinolinium hydroxide used as OSDA is given in Supplementary Information part 1 and the detailed synthesis procedure and the chemical compositions of the materials are given in Supplementary Information part 2.

The adsorption properties of the ITQ-29 materials were determined by Ar adsorption using a ASAP 2010 instrument from Micromeritics. Water and hydrocarbon adsorption capacities were determined on an IGA-3 gravimetric analyser from Hiden Isochema. Prior to the adsorption experiments the samples were outgassed at 400 °C for 12 h.

Structure refinement

The XRD patterns of the calcined ITQ-29 zeolites were measured at room temperature (22 °C) on a Philips X'Pert diffractometer with Bragg–Brentano geometry and an X'Celerator detector. Intensity data was obtained with a fixed divergence slit (0.25° for the Ge-containing sample and 0.125° for the pure-silica sample), Soller slits (incident and diffracted = 0.04° for the Ge-containing sample and 0.02° for the pure-silica sample) and Cu Kα radiation (λ = 1.5406, 1.5444 Å). Tube voltage and intensity, 45 kV and 40 mA; no secondary graphite monochromator. Step size was 0.017° = 2θ and time was 6,000 s for the Ge-containing sample and 1,450 s for the pure-silica sample.

The Rietveld refinement of Ge-ITQ-29 data was performed with program LSP7[25] using a 2θ range from 13.5° to 64.2°. Number of contributing reflections is 86. No geometric restraints used. Number of structural parameters is seven. Number of profile parameters is eight, including unit-cell parameters and zero shift (−0.020° 2θ) with visually estimated background (average background = 38.000 counts). Profile function used was Pearson VII. Refined overall thermal vibration coefficient $B = 6.0$ Å^2. The residuals of the refinement were $R_{wp} = 0.026$, $R_p = 0.018$, $\chi^2 = 5.0$.

The Rietveld refinement of the pure-silica ITQ-29 data with LSP7 was performed using the measured 2θ range from 5° to 75°. Number of contributing reflections is 186. No geometric restraints used. Number of structural parameters is seven. Number of profile parameters is eight, including unit-cell parameters and zero shift (−0.055° 2θ) with visually estimated background (average background = 400 counts). Profile function used was Pearson VII. Refined overall thermal vibration coefficient $B = 0.7$ Å^2. The residuals of the refinement were $R_{wp} = 0.097$, $R_p = 0.062$, $R_B = 0.032$, $\chi^2 = 2.8$.

Catalytic tests

Cracking of 1-hexene and 4-methyl-1-pentene using the calcined Al-ITQ-29 zeolite as catalyst was performed in a fixed-bed continuous reactor at atmospheric pressure, 773 K reaction temperature, 2.9 $g_{cat}\,g_{C6}^{-1}$ s contact time and 10 s time on stream.

The methanol into olefins reaction was carried out in a fixed-bed continuous reactor at 673 K, 0.14 bar of methanol and 58 h^{-1} weight hour space velocity using the calcined Al-ITQ-29 zeolite as catalyst.

Received 7 July; accepted 27 July 2004; doi:10.1038/nature02909.

1. Barrer, R. M. *Zeolites and Clay Minerals as Sorbents and Molecular Sieves* Ch. 1, 2 and 6 (Academic, London, 1978).
2. Breck, D. W. *Zeolite Molecular Sieves: Structure, Chemistry and Use* Ch. 1, 2 (John Wiley, New York, 1974).
3. Moscou, L. in *Introduction to Zeolite Science and Practice* (eds Van Bekkum, H., Flanigen, E. M. & Jansen, J. C.) Ch. 1 (Elsevier, Amsterdam, 1991).
4. Sherman, J. D. Synthetic zeolites and other microporous oxide molecular sieves. *Proc. Natl Acad. Sci. USA* **96,** 3471–3478 (1999).
5. Barrer, R. M., Denny, P. J. & Flanigen, E. M. Molecular sieve adsorbents. US patent 3,306,922 (1967).
6. Kerr, G. T. Synthetic zeolite. US patent 3,314,752 (1967).
7. Wadlinger, R. L., Rosinski, E. J. & Plank, C. J. Synthetic zeolite. US patent 3,375,205 (1968).
8. Kerr, G. T. Chemistry of crystalline aluminosilicates II. The synthesis and properties of zeolite ZK-4. *Inorg. Chem.* **5,** 1537–1539 (1966).
9. Kuehl, G. H. Shape selective catalyst from zeolite alpha and use thereof. US patent 4,299,686 (1981).
10. Gramlich, V. & Meier, W. M. The crystal structure of hydrated NaA: A detailed refinement of a pseudosymmetric zeolite structure. *Z. Kristallogr.* **133,** 134–149 (1971).
11. Gies, H. & Marler, B. The structure-controling role of organic templates for the synthesis of porosils in the system silica/template/water. *Zeolites* **12,** 42–49 (1992).
12. Lobo, R. F., Zones, S. I. & Davis, M. E. Structure-direction in zeolite synthesis. *J. Inclusion Phenom. Mol. Recogn. Chem.* **21,** 47–78 (1995).
13. Corma, A., Diaz-Cabañas, M. J., Rey, F., Nicolopoulus, S. & Boulahya, K. ITQ-15: The first ultralarge pore zeolite with a bi-directional pore system formed by intersecting 14- and 12-ring channels, and its catalytic implications. *Chem. Commun.* **12,** 1356–1357 (2004).
14. Corma, A., Díaz-Cabañas, M. J., Martínez-Triguero, L. J., Rey, F. & Rius, J. A large-cavity zeolite with wide pore windows and potential as an oil refining catalyst. *Nature* **418,** 514–517 (2002).
15. Corma, A., Rey, F., Valencia, S., Jordá, J. L. & Rius, J. A zeolite with interconnected 8-, 10- and 12-ring pores and its unique catalytic selectivity. *Nature Mater.* **2,** 493–497 (2003).
16. Castañeda, R., Corma, A., Fornés, V., Rey, F. & Rius, J. Synthesis of a new zeolite structure ITQ-24, with intersecting 10- and 12-membered ring pores. *J. Am. Chem. Soc.* **125,** 7820–7821 (2003).
17. Lee, H., Zones, S. I. & Davis, M. E. A combustion-free methodology for synthesizing zeolites and zeolite-like materials. *Nature* **425,** 385–388 (2003).
18. Nakano, T. & Yade, T. Synthesis, structure, and photophysical and electrochemical properties of a π-stacked polymer. *J. Am. Chem. Soc.* **125,** 15474–15484 (2003).
19. Blasco, T. *et al.* Preferential location of Ge in the double four-membered ring units of ITQ-7 zeolite. *J. Phys. Chem. B* **106,** 2634–2642 (2002).
20. Wang, Y., Song, J. & Gies, H. The substitution of germanium for silicon in AST-type zeolite. *Solid State Sci.* **5,** 1421–1433 (2003).
21. Olson, D. H., Camblor, M. A., Villaescusa, L. A. & Kuehl, G. H. Light hydrocarbon sorption properties of pure silica Si-CHA and ITQ-3 and high silica ZSM-58. *Micropor. Mesopor. Mater.* **67,** 27–33 (2004).
22. Barrett, P. A. *et al.* ITQ-12: a new microporous silica polymorph potentially useful for light hydrocarbon separations. *Chem. Commun.* 2114–2115 (2003).
23. Grande, C. A., Gigola, C. & Rodríguez, A. E. Adsorption of propane and propylene in pellets and crystals of 5A zeolite. *Ind. Eng. Chem. Res.* **41,** 85–92 (2002).
24. Boucheffa, Y. *et al.* Formation of carbonaceous compounds from propene and isobutene over a 5A zeolite. Influence of temperature on their compositions and locations. *Ind. Eng. Chem. Res.* **36,** 3198–3204 (1997).
25. Rius, J. *LSP7. A Computer Program for Restrained Rietveld Refinements* (Institut de Ciència de Materials de Barcelona-CSIC, Catalunya, 2002).

Supplementary Information accompanies the paper on **www.nature.com/nature**.

Acknowledgements We thank M. Benham and K. Gallimore at Hiden Isochema for carrying out the water and hydrocabon adsorption experiments. We also thank P. Atienzar and J. Martínez-Triguero for the photoluminescence and catalytic measurements, respectively. We are grateful to the CICYT for financial support.

Competing interests statement The authors declare that they have no competing financial interests.

Correspondence and requests for materials should be addressed to A.C. (acorma@itq.upv.es).